International Journal of Physics, 2023, Vol. 11, No. 1, 40-55
Available online at http://pubs.sciepub.com/ijp/11/1/5
Published by Science and Education Publishing
DOI:10.12691/ijp-11-1-5

Frustrated Spontaneous Emission near the Edge of a Photonic Band Gap

Mesfin Woldeyohannes*

Department of Chemistry & Physics, Western Carolina University,
112 Apodaca Science Building, Cullowhee, NC, USA, 28723
*Corresponding author: woldeyohan@email.wcu.edu

Received January 18, 2023; Revised February 20, 2023; Accepted March 02, 2023

Abstract The novel dynamical and spectral features of (single photon) spontaneous emission from an atomic transition near a photonic band edge are investigated by frustrating these features by spontaneous emission through another atomic transition far from the photonic band edge and deep in the photon continuum, the two atomic transitions forming the two dipole-allowed transitions of a three-level atom in a Λ configuration. Though spontaneous emission through the atomic transition far from the photonic band edge (the "far" transition) is not directly affected by the photonic band gap (PBG), it is indirectly affected by the PBG through its coupling to the atomic transition near the photonic band edge (the "near" transition) via the Λ configuration. As a result of this coupling, spontaneous emission through the "far" transition can be used as a probe to measure the strength of the effects of the PBG on spontaneous emission through the "near" transition. We have shown that the effects of the PBG on spontaneous emission via the "near" transition are strongly affected (and, therefore, can be controlled by) not only by the detuning of the "near" transition from photonic band edge but also by the vacuum decay rate of spontaneous emission through the "far" transition which is coupled to the "near" transition through the Λ configuration. In particular, we have shown that the oscillatory behavior of spontaneous emission near a photonic band edge as well as the Autler-Townes doublet of the spontaneous emission spectrum (due to the splitting of the atomic level near the photonic band edge) are strongly dependent on the decay rate of spontaneous emission through the probe transition which is far from the band edge.

Keywords: *photonic band gap materials, spontanoeous emission, three-level atom*

Cite This Article: Mesfin Woldeyohannes, "Frustrated Spontaneous Emission near the Edge of a Photonic Band Gap." *International Journal of Physics*, vol. 11, no. 1 (2023): 40-55. doi: 10.12691/ijp-11-1-5.

1. Introduction

The novel dynamical and spectral features of (single photon) spontaneous emission near the edge of a photonic band gap (PBG) are well known and are extensively discussed in the literature [1-6]. Chief among these novel feature of spontaneous emission near the edge of a PBG are its oscillatory behavior (as opposed to simple exponential decay in vacuum), and non-zero steady-state populations on excited levels (as opposed to zero in the case of vacuum) [6-9], leading to many actualized and potential applications such as enhancing the light extracting efficiency of LED's [10,11,12,13], improving photocatalysis [14,15], optical memory on atomic scale [8], qubits for quantum computation [9], super-radiance [16] as well as photon hopping conduction [17,18].

In this paper we apply a nearly exact operator formalism (the only approximations being electric dipole and rotating wave approximations) to investigate the dynamical and spectral features of (single photon) spontaneous emission from a three-level atom in a Λ configuration embedded in a PBG. Of the two dipole-allowed transitions of the three-level atom in a Λ configuration, one transition (the "near" transition) is close to the edge of the photonic band gap, whereas the other transition (the "far" transition) is far from the photonic band gap and deep in the photon continuum. As a result, spontaneous emission through the "near" transition is strongly affected by the photonic band gap, whereas that through the "far" transition is not directly affected by the it. However, even though the "far" transition is sufficiently far from the photonic band gap to be directly affected by it, it is indirectly affected by the gap because of its coupling to the "near" transition via the Λ configuration. As a result of this coupling, spontaneous emission through the "far" transition can be used as a probe to measure the strength of the effects of the photonic band gap on spontaneous emission through the "near" transition.

The atomic transition near the photonic band edge (the "near" transition) is characterized by its detuning from the band edge, whereas the atomic transition far from the photonic band gap and deep in the photon continuum (the "far" transition) is characterized by its vacuum decay rate. Our emphasis is on the combined effects of the detuning of the "near" transition from the photonic band edge, and

the vacuum decay rate of the "far" transition on the dynamics of spontaneous emission from the "near" transition. We have shown that the effects of the photonic band gap on spontaneous emission via the "near" transition are strongly affected (and, therefore, can be controlled by) not only by the detuning of the "near" transition from photonic band edge but also by the vacuum decay rate of the "far" transition which is coupled to the "near" transition through the Λ configuration. In particular, we have shown that the oscillatory behavior of spontaneous emission near a photonic band edge as well as the Autler-Townes doublet [19] of the spontaneous emission spectrum (due to the splitting of the atomic level near the photonic band edge as a result of the strong non-Markovian [16] interaction between the atom and its own localized radiation) are strongly dependent of the decay rate of the probe transition which is far from the band edge.

An arrangement of a Λ system in a PBG similar to ours has been briefly investigated by John and Quang [7]. However, their investigation was based on an isotropic dispersion model for the PBG which is but a non-realistic instructive toy model for studying the effects of a PBG qualitatively. Our detailed investigation in this paper is based on a realistic anisotropic dispersion model for the PBG which introduces several important quantitative corrections over and above the isotropic model [6].

This paper is organized as follows. In the next section (section 2) we describe our model system and write the Hamiltonian of the system under the electric dipole and rotating wave approximations [21]. In section 3, we write the general state vector of our model system in terms of the basis vectors of the Hamiltonian of the system as well as on time-dependent population amplitudes, and then derive the general solutions for these time-dependent amplitudes via the time-dependent Schödinger equation. In section 4, we introduce the memory kernels (delay Green's functions) describing the highly non-Markovian atom-photon interactions in PBG materials, for both isotropic and anisotropic dispersion models of a photonic band gap. Section 5 deals with detailed investigation of the dynamical and spectral behavior of spontaneous emission from our model Λ system under three subsections. Section 6 summarizes our conclusions. Finally, appendices A and B are used to derive the formulas employed in our investigation.

2. Model Hamiltonian

The physical system we consider consists of a single three-level atom embedded in a PBG material. We let |0> denote the ground level of the atom; and |1> and |2> the two excited levels, Figure 1. The three level atom is assumed to be in so called Λ configuration where the uppermost atomic level |2> is dipole coupled to the lower levels |1> and |0> by radiation modes (photon reservoir) in a three dimensional PBG, whereas the transition |1) → |0> is dipole forbidden.

We designate the energy of an atomic level $|i\rangle$ by $\hbar\omega_i$ and the frequency separation between level $|i\rangle$ and $|j\rangle$ by

$$\omega_{ij} = \omega_i - \omega_j \tag{2.1}$$

Transitions between atomic levels are described by atomic operators $\sigma_{ij} = |i\rangle\langle j|$ with the property $\sigma_{ij}|k\rangle = \delta_{jk}|i\rangle$ from which the commutation relation

$$\sigma_{ij}|k\rangle = |i\rangle\langle j| \Rightarrow \left[\sigma_{ij}, \sigma_{lk}\right] = \delta_{jl}\sigma_{ik} - \delta_{ik}\sigma_{lj} \tag{2.2}$$

readily follows. We let $\mathbf{d}$ denote the atomic dipole moment vector and express it in terms of the atomic operators σ_{ij} as

$$\mathbf{d} = \sum_{i,j} \mathbf{d}_{ij}\sigma_{ij}, \mathbf{d}_{ij} = \langle i|\mathbf{d}|j\rangle = d_{ij}\hat{\mathbf{d}}_{ij} \tag{2.3}$$

where d_{ij} is the magnitude of $\mathbf{d}_{ij}$, and $\hat{\mathbf{d}}_{ij}$ is the unit vector in the direction of $\mathbf{d}_{ij}$.

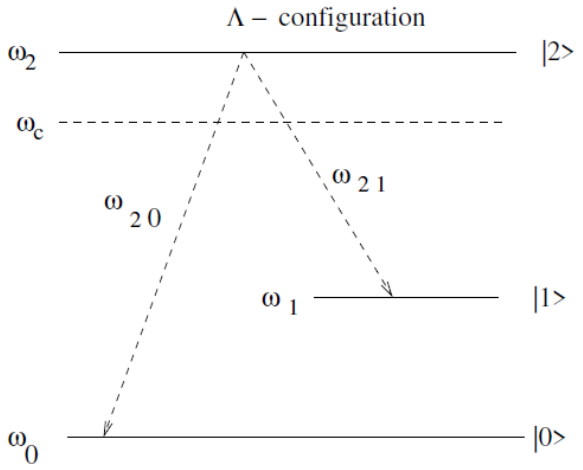

Figure 1. Three-level atom in a Λ configuration. The atomic transitions |2>→|0> and |2>→|1> are dipole-allowed transitions, whereas |1>→|0> is not. The atomic transition frequency ω_{20} is assumed to be near the band edge frequency ω_c of a PBG, whereas ω_{21} is far from the PBG and deep in the photonic continuum. For this reason, the atomic transitions |2>→|0> and |2>→|1> are dubbed, respectively, the "near" and the "far" transitions. The detuning of ω_{21} from ω_c is denoted by $\delta=\omega_{21}-\omega_c$

We assume that the atom is initially excited to the uppermost level $|2\rangle$ by a resonant laser pulse of frequency $\omega_L = \omega_{20}$. We then consider the scattering of this pulse via the transitions $|2\rangle \rightarrow |0\rangle$ and $|2\rangle \rightarrow |1\rangle$ into Rayleigh and Stokes components with frequencies $\omega_R = \omega_{20} = \omega_L$ and $\omega_S = \omega_{21} = \omega_L - \omega_{10}$. Accordingly, we divide the photon reservoir into two parts, a Raleigh part (identified by the subscript R) and a Stokes part (identified by the subscript S). With such a division, the Hamiltonian H describing our model atom-field system can be written as [6,20].

$$H = H_A + H_R + H_S + H_{AR} + H_{AS}, \tag{2.4}$$

where

$$H_A = \sum_{i=0}^{2} \hbar\omega_i\sigma_{ii}, \tag{2.5a}$$

$$H_R = \sum_{\lambda=1}^{2}\sum_{\mathbf{k}} \hbar\omega_k a^{\dagger}_{\mathbf{k}\lambda,R} a_{\mathbf{k}\lambda,R} \tag{2.5b}$$

$$H_S = \sum_{\lambda=1}^{2}\sum_{\mathbf{k}} \hbar\omega_k a^{\dagger}_{\mathbf{k}\lambda,S} a_{\mathbf{k}\lambda,S} \quad (2.5c)$$

$$H_{AR} = i\hbar \sum_{\lambda=1}^{2}\sum_{\mathbf{k}} g^{20}_{\mathbf{k}\lambda,R}(a^{\dagger}_{\mathbf{k}\lambda,R}\sigma_{02} - \sigma_{20}a_{\mathbf{k}\lambda,R}). \quad (2.5d)$$

$$H_{AS} = i\hbar \sum_{\lambda=1}^{2}\sum_{\mathbf{k}} g^{21}_{\mathbf{k}\lambda,S}(a^{\dagger}_{\mathbf{k}\lambda,S}\sigma_{12} - \sigma_{21}a_{\mathbf{k}\lambda,S}). \quad (2.5e)$$

Here H_A represents the Hamiltonian of the bare atom, whereas H_R and H_S represent, respectively, the Hamiltonians of the Rayleigh and Stokes components of the photon reservoir, $\mathbf{k}$ and λ being the wavevector and polarization index of a photon of mode $\{\mathbf{k}\lambda\}$. Associated with the Rayleigh and Stokes components are the annihilation ($a_{\mathbf{k}\lambda}$) and creation ($a^{\dagger}_{\mathbf{k}\lambda}$) operators satisfying the commutation rule

$$\left[a_{\mathbf{k}\lambda,\eta}, a^{\dagger}_{\mathbf{k}',\lambda',\eta'}\right] = \delta_{\eta\eta'}\delta_{\mathbf{k}\mathbf{k}'}\delta_{\lambda\lambda'}, \eta = R,S \quad (2.6)$$

whereby we assumed that the Rayleigh and Stokes components are well separated in frequency that their corresponding field operators commute. We also assume that atomic operators σ_{ij} commute with the field operators $a_{\mathbf{k}\lambda}$ and $a^{\dagger}_{\mathbf{k}\lambda}$ for the quantized Stokes and Rayleigh modes.

$$\left[\sigma_{ij}, a_{\mathbf{k}\lambda,\eta}\right] = \left[\sigma_{ij}, a^{\dagger}_{\mathbf{k}\lambda,\eta}\right] = 0, \eta = R,S \quad (2.7)$$

The Hamiltonians H_{AR} and H_{AS} given by Eqs. 2.5d and 2.5e are interaction Hamiltonians; H_{AR} describes interaction between the atom and the Rayleigh component of the photon reservoir, whereas H_{AS} describes the same between the atom and the Stokes component of the photon reservoir. These interaction Hamiltonians are written in the electric dipole approximation whereby the spatial variation of the photon field over the atom is ignored. They are also written in the rotating wave approximation whereby virtual processes of excitation (de-excitation) of the atom with simultaneous creation (annihilation) of a photon (terms of the form $a^{\dagger}_{\mathbf{k}\lambda}\sigma_{20}$ and $a_{\mathbf{k}\lambda}\sigma_{02}$) are neglected [21-25]. In these interaction Hamiltonians, the factors $g^{ij}_{\mathbf{k}\lambda,\eta}$ represent the frequency dependent coupling constants between the atomic transitions $|i\rangle \rightarrow |j\rangle$ and the modes $\{\mathbf{k}\lambda,\eta\}$ of the radiation field. These coupling constants are derived in [6] and are given by

$$g^{ij}_{\mathbf{k}\lambda,\eta} = \frac{\omega_{ij}d_{ij}}{\hbar}\left(\frac{\hbar}{2\epsilon_o\omega_{\mathbf{k}}V}\right)^{1/2}\hat{\mathbf{e}}_{\mathbf{k}\lambda,\eta}\cdot\hat{\mathbf{d}}_{ij}, \eta = R,S \quad (2.8)$$

where ω_{ij} is the atomic transition frequency given by Eq.2.1, d_{ij} and $\hat{\mathbf{d}}_{ij}$ are the magnitude and unit vector of the atomic dipole moment $\mathbf{d}_{ij}$ given by 2.3, V is the quantization volume of the radiation field, and ϵ_o is the Coulomb constant. The vectors $\hat{\mathbf{e}}_{\mathbf{k}\lambda,\eta}$ are the two transverse (polarization) unit vectors satisfying

$$\hat{\mathbf{k}}.\hat{\mathbf{e}}_{\mathbf{k}\lambda,\eta} = 0, \hat{\mathbf{e}}_{\mathbf{k}\lambda,\eta}.\hat{\mathbf{e}}_{\mathbf{k}\lambda',\eta} = \delta_{\lambda\lambda'}, \eta = R,S \quad (2.9)$$

where $\hat{\mathbf{k}}$ is the unit vector in the direction of the wavevector $\mathbf{k}$. The condition $\hat{\mathbf{k}}.\hat{\mathbf{e}}_{\mathbf{k}\lambda,\eta} = 0$ expresses transversality of the photon field, whereas the condition $\hat{\mathbf{e}}_{\mathbf{k}\lambda,\eta}.\hat{\mathbf{e}}_{\mathbf{k}\lambda',\eta'} = \boldsymbol{\delta}_{\lambda\lambda'}$ shows that unit vectors $\{\hat{\mathbf{e}}_{\mathbf{k}1,\eta}, \hat{\mathbf{e}}_{\mathbf{k}2,\eta}, \hat{\mathbf{k}}\}$ form a right-handed triad.

3. Excited State Population on Level |2> and Its Steady-State Value

For our model atom-field system, we assume that initially the atom is resonantly excited from the ground level $|0\rangle$ to the uppermost level $|2\rangle$ by a laser pulse of frequency $\omega_L = \omega_{20}$, whereas both the Rayleigh and Stokes components of the photon reservoir are in the vacuum state. As a result, the initial state of our model system can be written as the direct product of the atomic state $|2\rangle$ and the radiation state $|\{0\}\rangle$, since the atomic operators are assumed to commute with the radiation field operators (Eq. 2.7).

$$|\Psi(0)\rangle = |2,\{0\}\rangle \quad (3.1)$$

The notation $|2,\{0\}\rangle$ is a short way of writing the direct product state $|2\rangle|\{0\}\rangle$ which means the atom is in state $|2\rangle$ whereas both the Rayleigh and Stokes fields are in the vacuum state (that is, no Rayleigh or Stokes photons) [26].

As a result of the perturbation by the interaction Hamiltonians H_{AR} and H_{AS} applied at initial time $t = 0$, the initial state $|\Psi(0)\rangle$ of Eq. 3.1 evolves in time according to the time-dependent Schrödinger equation

$$i\hbar\frac{\partial}{\partial t}|\Psi(t)\rangle = H|\Psi(t)\rangle, \quad (3.2)$$

where H is the total Hamiltonian of the system given by Eq. 2.4. At any time t, the state vector of our model system can be written as a linear combination of the eigenstates of the non-interaction Hamiltonians H_A, H_R and H_S as

$$\begin{aligned}|\Psi(t)\rangle &= c_2(t)e^{-i\omega_2 t}|2,\{0\}\rangle \\ &+\sum_{\mathbf{k}\lambda} c_{\mathbf{k}\lambda,R}(t)e^{-i\left(\omega_{\mathbf{k},R}+\omega_0\right)t}|0,1_{\mathbf{k}\lambda,R}\rangle \\ &+\sum_{\mathbf{k}\lambda} c_{\mathbf{k}\lambda,S}(t)e^{-i\left(\omega_{\mathbf{k},S}+\omega_1\right)t}|1,1_{\mathbf{k}\lambda,S}\rangle\end{aligned} \quad (3.3)$$

where time dependencies due to H_A, H_R and H_S are explicitly factored out in the form of exponentials. The state vector $|0,1_{\mathbf{k}\lambda,R}\rangle$ means atom in state $|0\rangle$ and a single Rayleigh photon of mode $\{\mathbf{k}\lambda,R\}$. Similarly, the

state vector $|1,1_{\mathbf{k}\lambda,S}\rangle$ means atom in state $|1\rangle$ and a single Stokes photon of mode $\{\mathbf{k}\lambda,S\}$. From Eqs. (3.3) and (3.1), we obtain

$$c_2(0)=1,\ c_{\mathbf{k}\lambda,R}=c_{\mathbf{k}\lambda,S}(0)=0, \tag{3.4}$$

as the initial values for the amplitudes $c_2(t)$, $c_{\mathbf{k}\lambda,R}(t)$ and $c_{\mathbf{k}\lambda,S}(t)$ corresponding to the initial state (3.1).

Using Eq. 2.4 for the total Hamiltonian, and Eq. 3.3 for the general state vector in the Schrödinger equation (Eq. 3.2), and projecting the result onto the eigenstates $|2,\{0\}\rangle$, $|0,1_{\mathbf{k}\lambda,R}\rangle$ and $|1,1_{\mathbf{k}\lambda,S}\rangle$ of H_A, H_R and H_S, respectively, we obtain the following (infinite) set of coupled equations for the amplitudes $c_2(t)$, $c_{\mathbf{k}\lambda,R}(t)$ and $c_{\mathbf{k}\lambda,S}(t)$

$$\dot{c}_2(t)=-\sum_{\mathbf{k}\lambda}\begin{bmatrix} g^{20}_{\mathbf{k}\lambda,R}c_{\mathbf{k}\lambda,R}(t)e^{-i\mu_{\mathbf{k},R}t} \\ +g^{21}_{\mathbf{k}\lambda,S}c_{\mathbf{k}\lambda,S}(t)e^{-i\mu_{\mathbf{k},S}t}\end{bmatrix} \tag{3.5a}$$

$$\dot{c}_{\mathbf{k}\lambda,R}(t)=g^{20}_{\mathbf{k}\lambda,R}c_2(t)e^{i\mu_{\mathbf{k},R}t} \tag{3.5b}$$

$$\dot{c}_{\mathbf{k}\lambda,R}(t)=g^{21}_{\mathbf{k}\lambda,S}c_2(t)e^{i\mu_{\mathbf{k},S}t} \tag{3.5c}$$

Here a dot over an amplitude signifies total time derivative, whereas

$$\mu_{\mathbf{k},R}=\omega_{\mathbf{k},R}-\omega_{20},\ \mu_{\mathbf{k},S}=\omega_{\mathbf{k},S}-\omega_{21} \tag{3.6}$$

represent the detunings of the radiation mode frequencies $\omega_{\mathbf{k},R}$ and $\omega_{\mathbf{k},S}$ from the atomic transition frequencies ω_{20} and ω_{21}. Eqs. 3.5b and 3.5c can be integrated (in time), using the initial conditions (3.4), to give

$$c_{\mathbf{k}\lambda,R}(t)=g^{20}_{\mathbf{k}\lambda,R}\int_0^t c_2(t')e^{i\mu_{\mathbf{k},R}t'}dt'. \tag{3.7a}$$

$$c_{\mathbf{k}\lambda,S}(t)=g^{21}_{\mathbf{k}\lambda,S}\int_0^t c_2(t')e^{i\mu_{\mathbf{k},S}t'}dt'. \tag{3.7b}$$

Substituting these expressions for $c_{\mathbf{k}\lambda,R}(t)$, and $c_{\mathbf{k}\lambda,S}(t)$ in Eq. 3.5a and exchanging the order of summation over $\mathbf{k}\lambda$ and integration over time, we obtain the following integro-differential equation for $c_2(t)$.

$$\dot{c}_2(t)=-\int_0^t\left[G_R(t-t')+G_S(t-t')\right]c_2(t')dt' \tag{3.8}$$

Here

$$G_R(t-t')=\sum_{\mathbf{k}\lambda}\left(g^{20}_{\mathbf{k}\lambda,R}\right)^2e^{-i\mu_{\mathbf{k}\lambda,R}(t-t')} \tag{3.9a}$$

$$G_S(t-t')=\sum_{\mathbf{k}\lambda}\left(g^{21}_{\mathbf{k}\lambda,S}\right)^2e^{-i\mu_{\mathbf{k}\lambda,S}(t-t')} \tag{3.9b}$$

are the delay Green's functions associated with the Rayleigh and Stokes components of the photon reservoir, and depend very strongly on the photon density of states of the relevant photon reservoir. In essence, these Green's functions measure the photon reservoir's memory of its previous state at a later time and, therefore, are alternately known as memory kernels [6].

Our goal is to solve Eq. 3.8 for the amplitude $c_2(t)$ for different kinds of photon reservoirs which determine the nature of the Green's functions $G_R(t-t')$ and $G_S(t-t')$. The integral on the right hand side of Eq. 3.8 is a convolution integral which suggests solution by Laplace transformation [27]. Upon taking the Laplace transform of both sides of Eq. 3.8, and using the initial condition for $c_2(0)=1$ (Eq. 3.4), we obtain

$$\tilde{c}_2(s)=\frac{1}{s+\tilde{G}_R(s)+\tilde{G}_S(s)} \tag{3.10}$$

where $\tilde{c}_2(s)$, $\tilde{G}_R(s)$ and $\tilde{G}_S(s)$ are, respectively, the Laplace transforms of $c_2(t)$, $G_R(t)$, and $G_S(t)$. For given dispersion relations $\omega_{\mathbf{k},R}$ and $\omega_{\mathbf{k},S}$, we evaluate $G_R(t-t')$ and $G_S(t-t')$ from Eqs. 3.9 which, in turn, are used to evaluate $\tilde{G}_R(s)$ and $\tilde{G}_S(s)$. These expressions for $\tilde{G}_R(s)$ and $\tilde{G}_S(s)$ are then used in Eq. 3.10 to find $\tilde{c}_2(s)$. Finally, the amplitude $c_2(t)$ is obtained by inverting $\tilde{c}_2(s)$. Once $c_2(t)$ is calculated, the excited state population $n_2(t)$ on level $|2\rangle$, and the steady-state value n_{2s} of this excited state population are obtained from $c_2(t)$ by

$$n_2(t)=|c_2(t)|^2,\ n_{2s}=lim_{t\to\infty}|c_2(t)|^2 \tag{3.11}$$

4. Memory Kernels for Isotropic and Anisotropic PBG

The memory kernels (delay Green's functions) of Eqs. 3.9 for Rayleigh and Stokes photon reservoirs are highly dependent on the the dispersion relation for the relevant photon reservoir. In the case of vacuum, the dispersion relation is linear and is given by $\omega(k)=ck$, resulting in a density of propagating photon modes $\rho(\omega)$ which varies with frequency ω continuously like ω^2, Figure 2. For such a linear dispersion relation, the Green's functions of Eq. 3.9 are given by [6]

$$\begin{aligned} G_R(t-t')&=\gamma_{20}\delta(t-t'), \\ G_S(t-t')&=\gamma_{21}\delta(t-t')\end{aligned} \tag{4.1}$$

where

$$\gamma_{ij}=\frac{1}{4\pi\epsilon_o}\frac{4\omega_{ij}^3d_{ij}^2}{6\hbar c^3} \tag{4.2}$$

is one-half of the spontaneous emission rate Γ_{ij} for the transition $|i\rangle\to|j\rangle$, and $\delta(t-t')$ is the Dirac delta function.

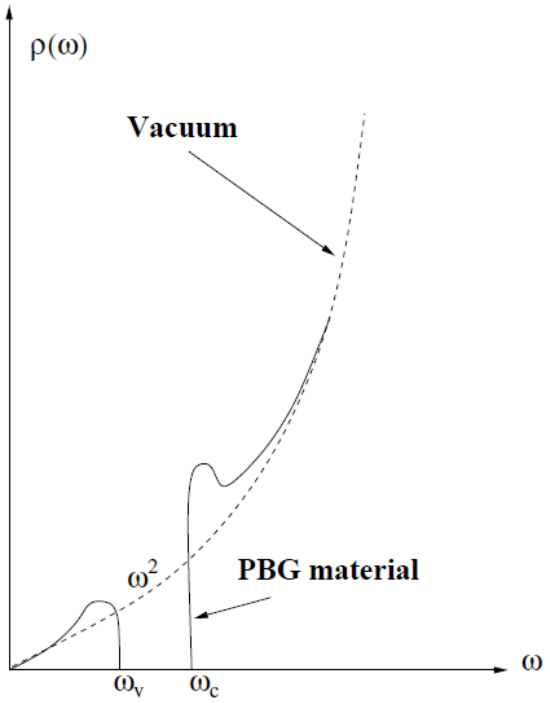

Figure 2. Density of propagating photon modes ρ(ω) for vacuum and for PBG as a function of frequency ω. In vacuum, ρ(ω) varies continuously like ω^2, whereas in a PBG, ρ(ω) exhibits a gap (or gaps) in which ρ(ω) is absolutely zero, ω_v and ω_c being the lower and upper band edge frequencies of the gap.

In free space, the memory kernels $G_R(t-t')$ and $G_S(t-t')$ are proportional to the delta function (Eq. 4.1). This is because free space is an infinitely broad photon reservoir (flat spectrum), and, therefore, its response should be instantaneous. Interactions governed by such delta function dependent memory kernels are said to be Markovian [22,23]. From Eq. 4.1, we obtain

$$\tilde{G}_R(s) = \gamma_{20}, \tilde{G}_S(s) = \gamma_{21} \tag{4.3}$$

for the Laplace transforms of the Green's functions in the case of vacuum.

In a PBG, unlike in vacuum, there is a gap (or gaps) in which the density of propagating photon modes $\rho(\omega)$ is absolutely zero [28], meaning photons with frequencies in the gap cannot propagate in the PBG, Figure 2. A simple model dispersion relation which exhibits a gap in the photon density of states is the so called isotropic effective mass dispersion relation given by [4,5]

$$\omega_{\mathbf{k}} \approx \omega_c + A(k-k_o)^2 \tag{4.4}$$

Here ω_c is the upper band edge frequency (Figure 2), k is the modulus of the wave vector $\mathbf{k}$, and k_o is a constant characteristic of the PBG. The factor A is a constant which measures the curvature of the dispersion curve $\omega(k)$ at $k = k_o$ and is given by

$$A = \frac{1}{2}\left(\frac{\partial^2\omega}{\partial k^2}\right)_{k=k_o} \approx \frac{\omega_c}{k_0^2} \approx \frac{c^2}{\omega_c} \tag{4.5}$$

The dispersion relation of Eq. 4.4 is valid only for frequencies close to the upper photonic band edge ω_c depicted in Figure 2. However, if the width $\omega_c - \omega_v$ of photonic band gap is large enough, and if the relevant atomic transitions are near enough the upper photonic band edge ω_c, the effects of the lower photonic band would be negligible, making Eq. 4.4 a good approximation.

The dispersion relation of Eq. 4.4 is isotropic because it depends only on the magnitude k of the wave vector $\mathbf{k}$. Such a dispersion relation associates the band edge wave vector with the entire sphere $|\mathbf{k}| = \mathbf{k_0}$ in k space (spherical Brillouin zone) and, therefore, artificially increases the true phase space available for photon propagation near the band edge. This results in a photonic density of states $\rho(\omega)$ which, near the band edge ω_c, behaves as $(\omega-\omega_c)^{-1/2}$ for $\omega > \omega_c$, the square-root singularity being characteristic of a one-dimensional phase space [4,5]. While there is no physical PBG material with isotropic gap, the isotropic dispersion relation of Eq. 4.4 gives qualitatively correct results. Realistic anisotropic dispersion relations lead only to quantitative corrections [6].

For the isotropic dispersion relation of 4.4, the Green's functions of Eq. 3.9 are given by [6]

$$G_R(t-t') = \beta_{20}^{3/2}\frac{e^{i[\delta_{20}(t-t')-\pi/4]}}{\sqrt{\pi(t-t')}}, \qquad \beta_{20}^{3/2} \approx \frac{1}{4}\left(\frac{\gamma_{20}}{\omega_{20}}\right)\omega_c^{3/2} \tag{4.6a}$$

$$G_S(t-t') = \beta_{21}^{3/2}\frac{e^{i[\delta_{21}(t-t')-\pi/4]}}{\sqrt{\pi(t-t')}}, \qquad \beta_{21}^{3/2} \approx \frac{1}{4}\left(\frac{\gamma_{21}}{\omega_{21}}\right)\omega_c^{3/2} \tag{4.6b}$$

where

$$\delta_{20} = \omega_{20} - \omega_c, \delta_{21} = \omega_{21} - \omega_c \tag{4.7}$$

represent the detunings of the atomic transition frequencies ω_{20} and ω_{21} from the upper band edge frequency ω_c. At optical frequencies $\gamma_{ij} \sim 10^8\,Hz$ and $\omega_{ij} \sim 2\pi\times10^{15}\,Hz$ so that $\beta_{ij} \sim 10^{-6}\omega_c$. Thus, if the band-edge ω_c is also in the optical regime, we have $\beta_{ij} \sim 10^{10}\,Hz$.

Eq. 4.6 shows that, in the case of an isotropic PBG, the memory kernels $G_\eta(t-t')$ decay in time like $(t-t')^{-1/2}$, unlike in the case free space where the $G_\eta(t-t')$ have delta function time dependence (Eq. 4.1). As a result, unlike in the case of vacuum where atom-photon interaction is Markovian [22,23], in the case of PBG, atom-photon interactions are highly non-Markovian [16]. From Eqs.4.6, we obtain

$$\tilde{G}_R(s) = \frac{-(i\beta_{20})^{3/2}}{\sqrt{s-i\delta_{20}}}, \tilde{G}_S(s) = \frac{-(i\beta_{21})^{3/2}}{\sqrt{s-i\delta_{21}}} \tag{4.8}$$

for the Laplace transforms of the green's functions in the case of isotropic PBG.

In a real 3D PBG, the gap is highly anisotropic and the band edge is associated with a finite collection of symmetry related points in k space, rather than with the entire sphere $|\mathbf{k}|=|\mathbf{k_o}|$. For such a realistic PBG, the effective mass approximation of the photon dispersion relation near the upper band edge takes the vector form [4,5]

$$\omega_{\mathbf{k}} \approx \omega_c + A(\mathbf{k}-\mathbf{k}_o)^2. \tag{4.9}$$

In this case A, is approximately given by $A \approx fc^2/\omega_c$ where f is a dimensionless factor for scaling the different slopes the dispersion curve exhibits in different directions. The anisotropic dispersion relation of Eq. 4.9 leads to a photonic density of states which behaves as $\rho(\omega) \sim (\omega-\omega_c)^{1/2}$ for $\omega > \omega_c$, characteristic of a three-dimensional phase space [4,5].

For the anisotropic dispersion relation of 4.9, the Green's functions of Eq. 3.9 are given by [6]

$$G_R(t-t') = -\alpha_{20}\frac{e^{i[\delta_{20}(t-t')+\pi/4]}}{\sqrt{4\pi(t-t')^3}}, \qquad \alpha_{20}^2 \approx \frac{1}{16f^3}\left(\frac{\gamma_{20}}{\omega_{20}}\right)^2\omega_c \tag{4.10a}$$

$$G_S(t-t') = -\alpha_{21}\frac{e^{i[\delta_{21}(t-t')+\pi/4]}}{\sqrt{4\pi(t-t')^3}}, \qquad \alpha_{21}^2 \approx \frac{1}{16f^3}\left(\frac{\gamma_{21}}{\omega_{21}}\right)^2\omega_c \tag{4.10b}$$

where δ_{20} and δ_{21} are detuning frequencies given by Eq. 4.7, whereas γ_{ij} (given by Eq. 4.2) is one-half of the spontaneous emission rate Γ_{ij} for the transition $|i\rangle \rightarrow |j\rangle$. At optical frequencies, $\gamma_{ij} \sim 10^8\,Hz$ and $\omega_{ij} \sim 2\pi\times 10^{15}\,Hz$ so that $\alpha_{ij}^2 \sim 10^{-17} f^{-3}\omega_c$. For example, when $f = 10^3$, we obtain $\alpha^2 \sim 10^{-8}\omega_c$ so that $\alpha^2 \sim 10^7\,Hz$, for ω_c is in the optical regime.

Eqs. 4.10 show that, for the anisotropic dispersion relation of Eq. 4.9, the memory kernels decay in time faster like $(t-t')^{-3/2}$ as opposed to the slower $(t-t')^{-1/2}$ time decay for the isotropic dispersion relation of Eq. 4.4. The enhanced memory effect for the isotropic model is an artifact of artificially increasing the phase space available for propagating photon modes near the upper band edge by associating the band edge with an entire sphere $|\mathbf{k}|=\mathbf{k_0}$ in k space rather than with a finite collection of symmetry-related points. From Eqs. 4.10, we obtain

$$\tilde{G}_R(s) = \alpha_{20}e^{i\pi/4}\sqrt{s-i\delta_{20}}, \qquad \tilde{G}_S(s) = \alpha_{21}e^{i\pi/4}\sqrt{s-i\delta_{21}} \tag{4.11}$$

for the Laplace transforms of the green's functions in the case of anisotropic PBG.

5. Spontaneous Emission from A Λ System in a PBG

When the three-level atom in the Λ configuration is in vacuum, we use Eq. 4.3 in Eq. 3.10 to obtain

$$\tilde{c}_2(s) = \frac{1}{s+\gamma_{20}+\gamma_{21}} \tag{5.1}$$

which can be easily inverted to give

$$c_2(t) = e^{-(\gamma_{21}+\gamma_{21})t} \tag{5.2}$$

showing that, in the case of vacuum, spontaneous emission from level $|2\rangle$ is purely exponential, and that, in the stead-state (long-time) limit, the population of the excited level $|2\rangle$ is zero. That spontaneous emission is purely exponential, and that all populations on excited levels eventually decay to the ground level is a general result valid not only for vacuum but for any broadband smoothly varying electromagnetic density of states in which the Wigner-Weisskopf approximation is valid [25].

When the electromagnetic density of states changes abruptly in the vicinity of an atomic transition (such as near a photonic band edge), spontaneous emission through the transition displays behaviors dramatically different from those in vacuum. In particular, spontaneous emission near a photonic band edge is shown to be oscillatory (as opposed to simple exponential decay in vacuum), and there may be non-zero (fractionalized) steady-state population in excited states unlike in the case of vacuum in which all excited state populations eventually decay to the ground level [6,7,8,9].

The case of spontaneous emission from a three-level atom in the Λ configuration embedded in a PBG material modeled by the isotropic dispersion relation of Eq. 4.4 is briefly discussed in [7]. In this work, we discuss the same case in much more detail, with the PBG modeled by the more realistic anisotropic dispersion relation of Eq. 4.9 which gives quantitative corrections over and above the isotropic model.

In our analysis of the three-level atom in the Λ configuration, we make two important assumptions. The first assumption is that the Stokes frequency ω_{21} lies in the photon continuum far outside the gap so that atom-photon interaction for the transition $|2\rangle \rightarrow |1\rangle$ is described by the vacuum memory kernel of Eq. 4.1 for which the Laplace transform is given by $\tilde{G}_S(s) = \gamma_{21}$ (Eq. 4.3). The second assumption is that the Rayleigh frequency ω_{20} lies near the photonic band edge ω_c so that atom-photon interaction for the transition $|2\rangle \rightarrow |0\rangle$ is described by the anisotropic PBG memory kernel of Eq. 4.10b for which the Laplace transform is given by Eq. 4.11. Applying these two assumptions in Eq. 3.10, we obtain

$$\tilde{c}_2(s+i\delta) = \frac{1}{D(s)} \tag{5.3}$$

where

$$D(s) = s + \alpha_{20}e^{i\pi/4}\sqrt{s} + (\gamma_{21}+i\delta) \tag{5.4}$$

Substituting $x = e^{-i\pi/4}\sqrt{s}$ in the equation for $D(s)$, we obtain

$$D(s) = iD(x) \tag{5.5}$$

where

$$D(x) = x^2 + \alpha_{20}x + (\delta - i\gamma_{21}) \tag{5.6}$$

is a quadratic equation whose roots (separated into real and imaginary parts) are given by

$$q_{1,2} = \left[-\left(\frac{\alpha_{20}}{2}\right) \pm \sqrt{\frac{\sqrt{\eta^2 + \gamma_{21}^2} + \eta}{2}} \right] \pm i\sqrt{\frac{\sqrt{\eta^2 + \gamma_{21}^2} - \eta}{2}} \tag{5.7}$$

where

$$\eta = \left(\frac{\alpha_{20}}{2}\right)^2 - \delta \tag{5.8}$$

In terms of the roots of $D(x) = 0$, Eq. 5.4 for $D(s)$ is expressed as

$$\begin{aligned} D(s) &= s + \alpha_{20}e^{i\pi/4}\sqrt{s} + (\gamma_{21} + i\delta) \\ &= \prod_{j=1}^{2} (\sqrt{s} - e^{i\pi/4} q_j). \end{aligned} \tag{5.9}$$

Using Eq. 5.9 in Eq. 5.3, we obtain

$$\begin{aligned} \tilde{c}_2(s + i\delta) &= \frac{1}{s + \alpha_{20}e^{i\pi/4}\sqrt{s} + (\gamma_{21} + i\delta)} \\ &= \frac{1}{\prod_{j=1}^{2}\left(\sqrt{s} - e^{i\pi/4} q_j\right)} \end{aligned} \tag{5.10}$$

The amplitude $c_2(t)$ is obtained from the inverse Laplace transforms of $\tilde{c}_2(s + i\delta)$ given by Eq. 5.10 via the complex inversion formula [27]

$$e^{-i\delta t} c_2(t) = \frac{1}{2\pi i}\int_{\epsilon - i\infty}^{\epsilon + i\infty} e^{st}\tilde{c}_2(s + i\delta)ds, \tag{5.11}$$

where the real number ϵ is chosen so that $s = \epsilon$ lies to the right of all the singularities (poles and branch points) of the function $\tilde{c}_2(s + i\delta)$. Once $c_2(t)$ is calculated, the excited state population $n_2(t)$ on level $|2\rangle$ as well as the steady-state value n_{2s} of this excited state population are obtained from $c_2(t)$ via Eq. 3.11.

Our objective in this work is to evaluate $c_2(t)$ for a PBG described by the anisotropic dispersion relation of Eq. 4.9, and then investigate the nature and behavior of the excited state population $n_2(t)$ as well as its steady-state value n_{2s} for such a dispersion relation. To this end, we consider the case in which $\gamma_{21} = 0$ separately from the case in which $\gamma_{21} \neq 0$ in the following subsections.

5.1. Spontaneous Emission near the Edge of an Anisotropic PBG: the γ_{21}= 0 Case

Our system of three-level atom in the Λ configuration depicted in Figure 1 is initially assumed to be in the upper most level $|2\rangle$ (Eq. 3.4). If we further assume that $\gamma_{21} = 0$, the decay channel $|2\rangle \to |1\rangle$ for the initial population on level $|2\rangle$ is completely closed, so that the three-level atom essentially acts as a two-level atom consisting of atomic levels $|2\rangle$ and $|0\rangle$. This case of spontaneous emission from a two-level atom near the edge of a photonic band gap has been discussed in detail in [7], albeit under the non-realistic isotropic dispersion of Eq. 4.4. In this subsection, we briefly discuss this two-level atom case under the realistic anisotropic dispersion relation of Eq. 4.9. This $\gamma_{21} = 0$ case involving only two of the three atomic levels, besides being an interesting case in its own right, will be used as a reference for the $\gamma_{21} \neq 0$ case, whereby all three levels of the three-level atom have to be taken into consideration.

For $\gamma_{21} = 0$, Appendix B shows that the amplitude $c_2(t)$ is given by

$$\gamma_{21} = 0 \Rightarrow$$

$$c_2(t) = \begin{cases} \dfrac{2u_1}{u_1 - u_2} e^{i(u_1^2 + \delta)t} + I(\delta, t), \text{ if } \delta < 0 \\ I(\delta, t, \text{ if } 0 \le \delta \le (\alpha_{20}/2)^2 \\ \dfrac{2v_2}{v_2 - v_1} e^{i(v_2^2 + \delta)t} + I(\delta, t), \text{ if } \delta > (\alpha_{20}/2)^2 \end{cases} \tag{5.12}$$

where

$$u_{1,2} = -\left(\frac{\alpha_{20}}{2}\right) \pm \sqrt{|\delta| + \left(\frac{\alpha_{20}}{2}\right)^2} \tag{5.13a}$$

$$v_{1,2} = -\left(\frac{\alpha_{20}}{2}\right) \pm i\sqrt{|\delta| - \left(\frac{\alpha_{20}}{2}\right)^2} \tag{5.13b}$$

the upper signs of $\pm$ applying for u_1 and v_1. The term $I(\delta, t)$ is given by

$$I(\delta, t) = \frac{\alpha_{20}e^{i\pi/4}}{\pi}\int_0^\infty \frac{\sqrt{x}e^{-(x - i\delta)t}}{(-x + i\delta)^2 + i\alpha_{20}^2 x} dx \tag{5.14}$$

and represents the branch-cut contribution arising from the deformation of the contour of integration around a branch point in the complex inversion of Eq. 5.10 via Eq. 5.11.

From the population amplitude $c_2(t)$ given by Eq. 5.12, the excited state population $n_2(t)$ on level $|2\rangle$ is obtained by $n_2(t) = |c_2(t)|^2$ (according to Eq. 3.11. This excited state population on level $|2\rangle$ is depicted Figure 3 as a function of the scaled time $\alpha_{20}^2 t$ for various values of the detuning parameter $\delta = \omega_{20} - \omega_c$. From this figure we see that, unlike in the case of vacuum where spontaneous emission decay is purely exponential, spontaneous emission near the edge of a photonic band gap exhibits pronounced oscillatory behavior [7]. This oscillatory behavior of spontaneous emission near a photonic band edge was first predicted by John and Quang [7] using the isotropic dispersion model of Eq. 4.4. Our result depicted in Figure 3 confirms their result for the more realistic anisotropic dispersion model of Eq. 4.9.

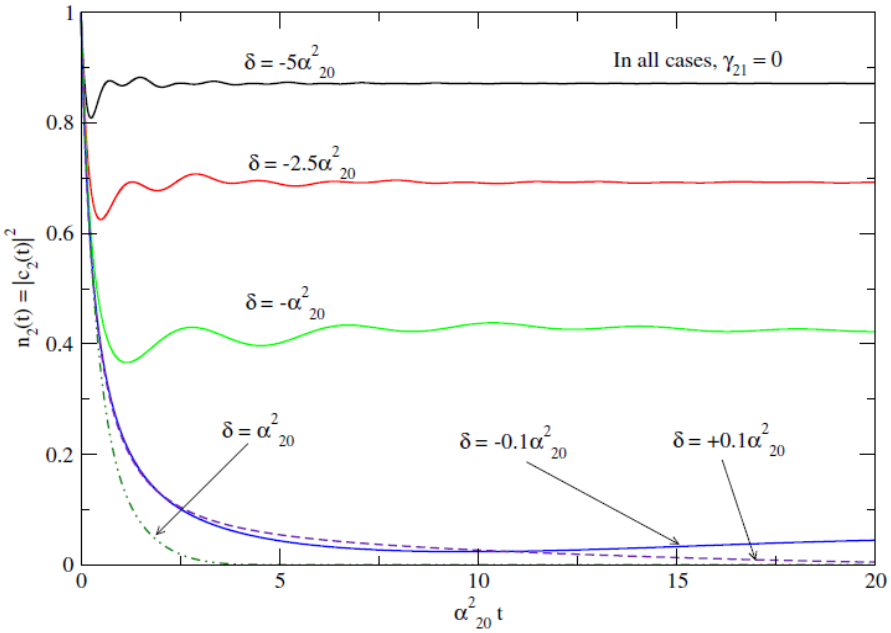

Figure 3. Atomic population $n_2(t) = |c_2(t)|^2$ on level $|2\rangle$ for $c_2(t)$ given by Eq. 5.12 as a function of the scaled time $\alpha^2_{20}t$, for $\gamma_{21} = 0$ and for various values of δ, the PBG described by the anisotropic dispersion relation of Eq. 4.9

Besides its oscillatory behavior, the other novel feature of spontaneous emission near a photonic band edge is the presence of non-zero (fractionalized) steady-state population on the excited level $|2\rangle$, as opposed to zero in the case of vacuum. This feature of spontaneous emission was first predicted again by John and Qaung [7], and again for the case of the isotropic dispersion relation of Eq. 4.4. We hereby have shown that their prediction is also true for the more realistic anisotropic dispersion relation of Eq. 4.9, albeit with one major difference. For the case of the isotropic dispersion relation, non-zero steady-state population on an excited level was predicted even when the excited level lies slightly outside the gap but not far from it [7]. However, for the case of anisotropic dispersion relation, non-zero steady-state population exists on an excited level only when the level is strictly inside the gap so that its detuning $\delta = \omega_{21} - \omega_c$ from the band edge ω_c is negative. This discrepancy between the two dispersion relations is due to the enhanced memory effect of the isotropic one which varies as $t^{-1/2}$ (according to Eq. 4.6) as opposed to that of the anisotropic one which varies as $t^{-3/2}$ (according to Eq. 4.10).

For the $\gamma_{21} = 0$ case, Appendix B shows that the steady-state value of the excited state population on level $|2\rangle$ is given by

$$\gamma_{21} = 0 \Rightarrow n_{2s} = \lim_{t\to\infty} |c_2(t)|^2 = \begin{cases} \dfrac{4u_1^2}{(u_1 - u_2)^2}, & \text{if } \delta < 0 \\ 0, & \text{if } \delta \geq 0 \end{cases} \quad (5.15)$$

where $u_{1,2}$ are given by Eq. 5.13a. Therefore, even when the excited level $|2\rangle$ is right on the band edge so that $\delta = \omega_{20} - \omega_c = 0$, there is no excited population on level $|2\rangle$ in the steady-state limit. The variation of this steady-state population of level $|2\rangle$ according to Eq. 5.15 is depicted in Figure 4.

5.2. Frustrated Spontaneous Emission near the Edge of an Anisotropic PBG: the $\gamma_{21} \neq 0$ Case

For the $\gamma_{21} \neq 0$ case, Appendix A shows that $c_2(t)$ is given by

$$c_2(t) = \frac{2q_1}{q_1 - q_2} e^{i(q_1^2 + \delta)t} + \frac{2q_2}{q_2 - q_1} e^{i(q_2^2 + \delta)t} + I(\delta, t) \quad (5.16)$$

where $q_{1,2}$ are given by Eq. 5.7, and

$$I(\delta, t) = \frac{\alpha_{20} e^{i\pi/4}}{\pi} \int_0^\infty \frac{\sqrt{x} e^{-(x - i\delta)t}}{(-x + i\delta + \gamma_{21})^2 + i\alpha_{20}^2 x} dx \quad (5.17)$$

represents the branch-cut contribution of the complex inversion of Eq. 5.10.

Figure 1 depicts the variations of the excited state population $n_2(t) = |c_2(t)|^2$ of level $|2\rangle$ for $c_2(t)$ given by Eq. 5.16 as a function of the scaled time $\alpha_{20}^2 t$ for various values of the detuning parameter $\delta = \omega_{20} - \omega_c$. From this figure we see that, like in the $\gamma_{21} = 0$ case, in the $\gamma_{21} \neq 0$ case the spontaneous decay of the excited state population displays strong oscillatory behavior. However, unlike in the $\gamma_{21} = 0$ case, in the $\gamma_{21} \neq 0$ case all excited state population eventually decays to the ground level in the long-time (steady-state) limit, even when the excited level lies deep inside the photonic band gap. This total decay in the excited population of level $|2\rangle$ occurs through decay channel $|2\rangle \to |1\rangle$ which is assumed to be far outside the gap and deep in the photon continuum.

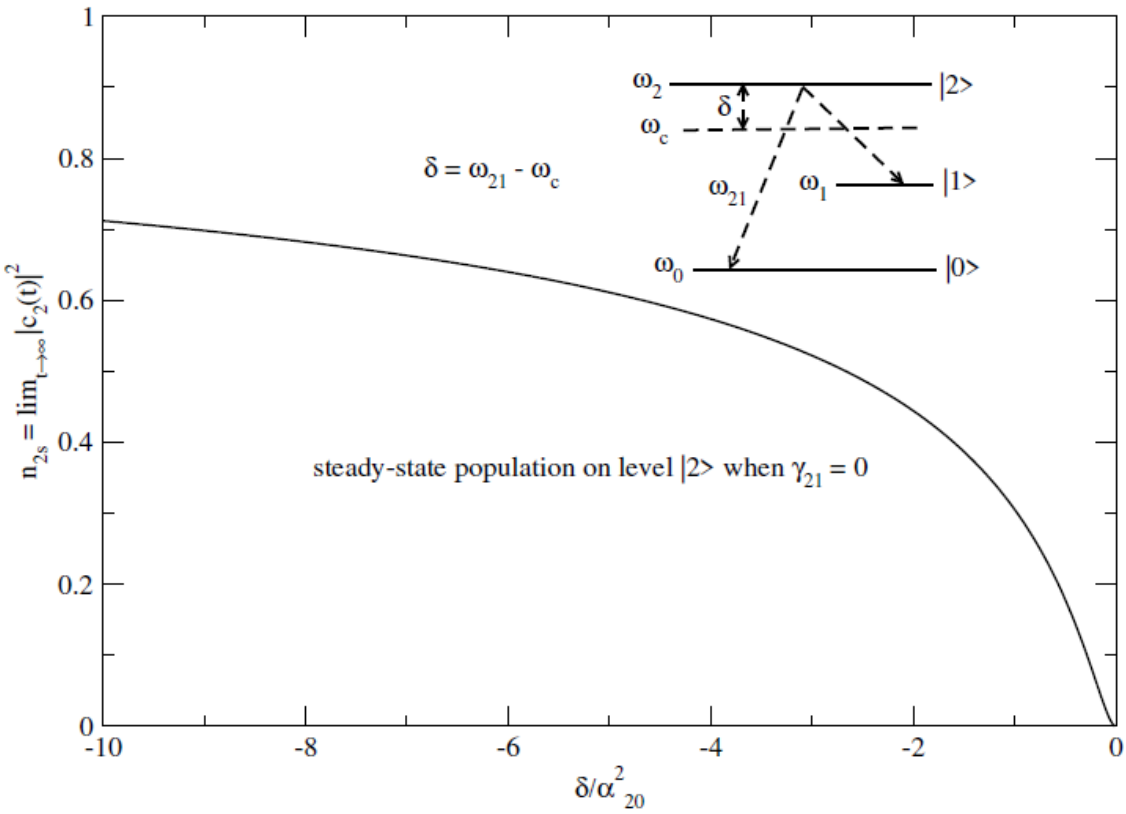

Figure 4. Steady-state population on the excited level |2> as given by Eq. 5.15 as a function of the scaled detuning δ/α^2_{20}, when $\gamma_{21} = 0$ and the PBG is described by the anisotropic dispersion relation of Eq. 4.9. Unlike the isotropic dispersion of Eq. 4.4 for which steady-state population on an excited level was predicted to be non-zero even when the atomic transition lies outside the gap [7], for the more realistic anisotropic dispersion relation, the steady-state population on an excited level is non-zero only when the corresponding atomic transition of the level lies inside the gap so that $\delta < 0$

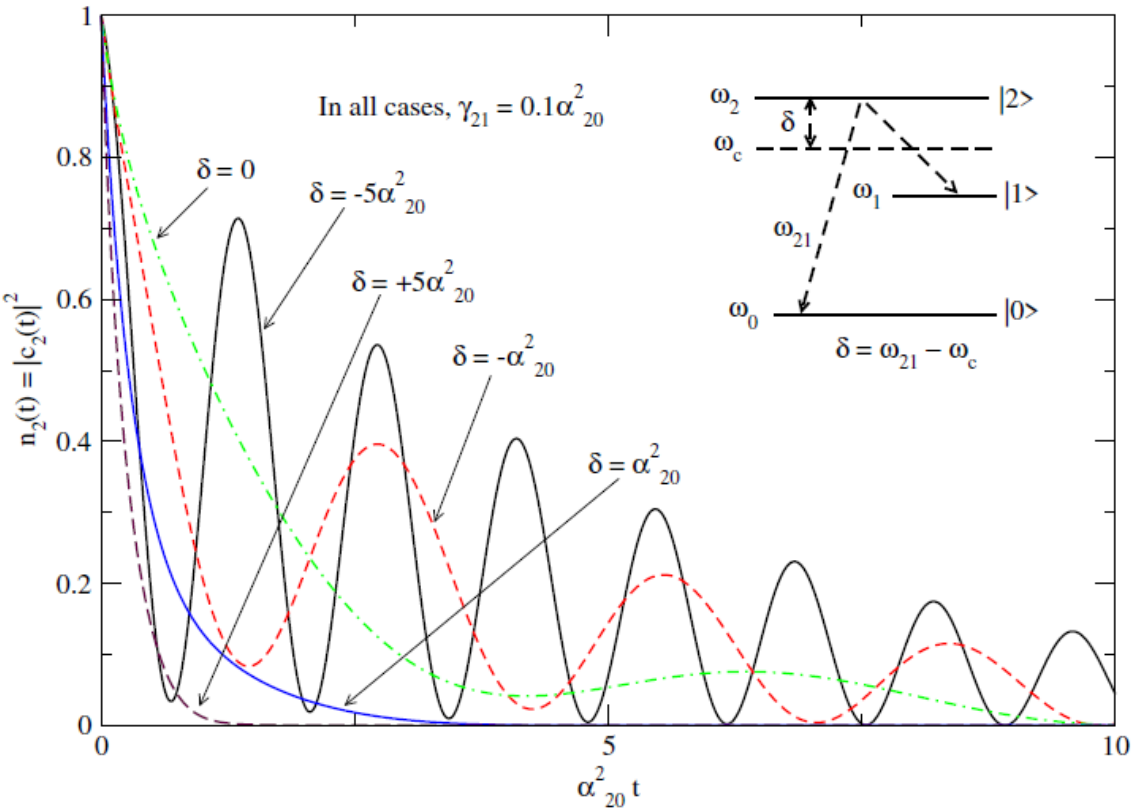

Figure 5. Atomic population $|c_2(t)|^2$ on level |2> for $c_2(t)$ given by Eq. 5.16 as a function of the scaled time $\alpha^2_{20}t$, for $\gamma_{21} = 0.1\alpha^2_{20}$ and for various values of δ, the PBG described by the anisotropic dispersion relation of Eq. 4.9. When $\gamma_{21} \neq 0$, the excited state population always decays to zero sooner or later depending on the value of δ

We can easily see why the steady-state population on the exited level $|2\rangle$ is always zero when $\gamma_{21} \neq 0$, by investigating the three terms on the RHS of Eq. 5.16. Since $\alpha_{20}^2 \sim 10^7\, Hz$ and $\gamma_{21} \sim 10^8\, Hz$ at optical frequencies, from Eq. 5.7 we see that the real and imaginary parts of root u_1 are both positive whereas those of root u_2 are both negative. Therefore, the roots u_1 and u_2 can be expressed as

$$q_1 = A_1 + iB,\ q_2 = -(A_2 + iB) \tag{5.18}$$

where $A_{1,2}$ and B are positive real numbers given by

$$A_1 = -\left(\frac{\alpha_{20}}{2}\right) + \sqrt{\frac{\sqrt{\eta^2 + \gamma_{21}^2} + \eta}{2}} > 0 \tag{5.19a}$$

$$A_2 = \left(\frac{\alpha_{20}}{2}\right) + \sqrt{\frac{\sqrt{\eta^2 + \gamma_{21}^2} + \eta}{2}} > 0 \tag{5.19b}$$

$$B = \sqrt{\frac{\sqrt{\eta^2 + \gamma_{21}^2} - \eta}{2}} > 0 \tag{5.19c}$$

As a result, the exponentials on the RHS of Eq. 5.16 involving the roots $\hbar\omega_i$ and $\hbar\omega_i$ can be cast as

$$e^{i(q_1^2+\delta)t} = e^{i(A_1^2 - B^2 + \delta)t} e^{-2A_1 Bt} \tag{5.20a}$$

$$e^{i(q_2^2+\delta)t} = e^{i(A_2^2 - B^2 + \delta)t} e^{-2A_2 Bt} \tag{5.20b}$$

showing that the first two terms on the RHS of Eq. 5.16 are both oscillatory due to the factors $e^{i(A_1^2 - B^2 + \delta)t}$ and $e^{i(A_2^2 - B^2 + \delta)t}$ but both decay to zero in the steady-state limit ($t \to \infty$) due to the factors $e^{-2A_1 Bt}$ and $e^{-2A_2 Bt}$. Moreover, the integrand on the RHS Eq. 5.16 decays to zero as e^{-xt}. It follows that all three terms on RHS of Eq. 5.16 decay to zero as $t \to \infty$, so that the amplitude $c_2(t)$ and, therefore, the population $|c_2(t)|^2$ decay to zero in the steady-state limit.

The oscillatory behavior of the excited state population $n_2(t) = |c_2(t)|^2$ on level $|2\rangle$ (which is assumed to be near the photonic band edge ω_c) depends on the strength of the decay channel $|2\rangle \to |1\rangle$ which is specified by the decay parameter γ_{21}. As shown in Figure 6, the smaller the value of γ_{21}, the slower the decay of $n_2(t)$ and the longer the oscillation life-time of $n_2(t)$, though the oscillation frequency of $n_2(t)$ depends only on the value of δ. The ability to control the oscillatory behavior of spontaneous emission near the edge of a photonic band gap using γ_{21} as depicted in Figure 6 is an important conclusion of our investigation.

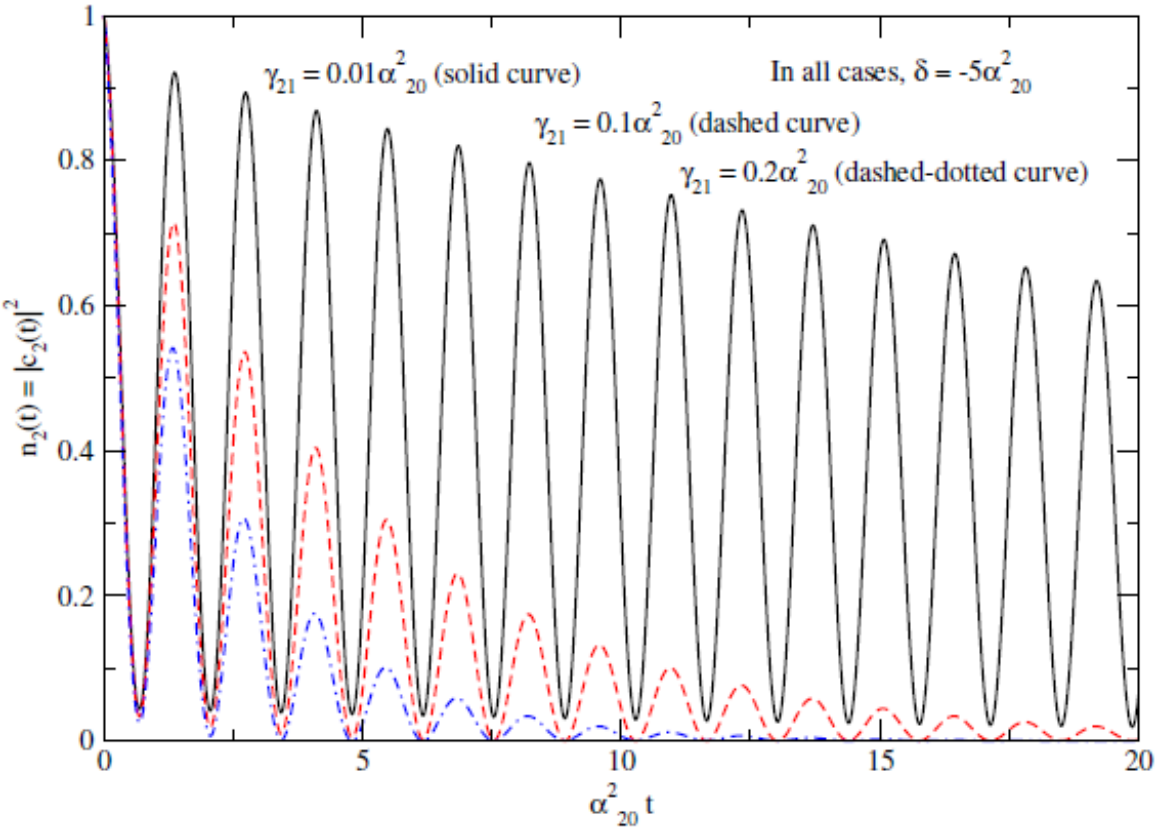

Figure 6. Atomic population $|c_2(t)|^2$ on level |2> for $c_2(t)$ given by Eq. 5.16 as a function of the scaled time $\alpha^2_{20}t$, for $\delta = -5\alpha^2_{20}$ and for various values of γ_{21}, the PBG described by the anisotropic dispersion relation of Eq. 4.9. The smaller the value of γ_{21}, the longer the oscillation life-time of the population of level |2>, though the frequency of oscillation depends only on δ

5.3. Spectrum of Frustrated Spontaneous Emission near the Edge of an Anisotropic PBG

With $\tilde{c}_2(s)$ given by Eq. 5.10, the spectrum of the spontaneous emission through the decay channel $|2\rangle \rightarrow |1\rangle$ is given by [7]

$$S(\omega_\lambda) \sim \left|\tilde{c}_2\left[-i\left(\omega_\lambda - \omega_{21}\right)\right]\right|^2 = \left|\frac{1}{-i(\omega_\lambda - \omega_{21}) - \alpha_{20}\sqrt{(\omega_\lambda - \omega_{21}) + \delta} + \gamma_{21}}\right|^2 \quad (5.21)$$

Figure 7 depicts the spectrum $S(\omega_\lambda)$ for $\gamma_{21} = \alpha_{20}^2$ and for different values of the detuning $\delta = \omega_{20} - \omega_c$ of the atomic transition frequency ω_{20} from the band edge frequency ω_c. From this figure we see that for small δ (that is, when level $|2\rangle$ is close to the band edge) the spectrum $S(\omega_\lambda)$ splits into a doublet. This splitting is analogous to the Autler-Townes splitting (dynamic Stark splitting) of an excited level into two dressed states by a resonant (or nearly resonant) external driving field. In the PBG case, however, there is no external driving field, and the splitting is solely due to the strong non-Markovian interaction of the atom with its localized radiation field [1,2,14]. This splitting was first predicted by John and Quang [7], albeit for a PBG described by the isotropic dispersion relation of Eq. 4.4 which artificially enhances the effects of the PBG by artificially increasing the phase space available for band edge photons. The splitting depicted in Figure 7 is for a PBG describe by the more realistic anisotropic relation of Eq. 4.9 and, therefore, is not as pronounced as that in [7].

Figure 8 depicts the spectrum $S(\omega_\lambda)$ for $\delta = \alpha_{20}^2$, and for different values of the decay rate γ_{21} of the spontaneous emission through the transition $|2\rangle \rightarrow |1\rangle$ which is assumed to be sufficiently far from the gap to be directly affected by the gap. From this figure, we see that the smaller the value of γ_{21} the more pronounced the splitting effect on $S(\omega_\lambda)$, though the positions of the peaks is determined only by δ. The ability to control the spectrum of spontaneous emission near the edge of a photonic band gap using γ_{21} as depicted in Figure 8 is another important conclusion of our investigation.

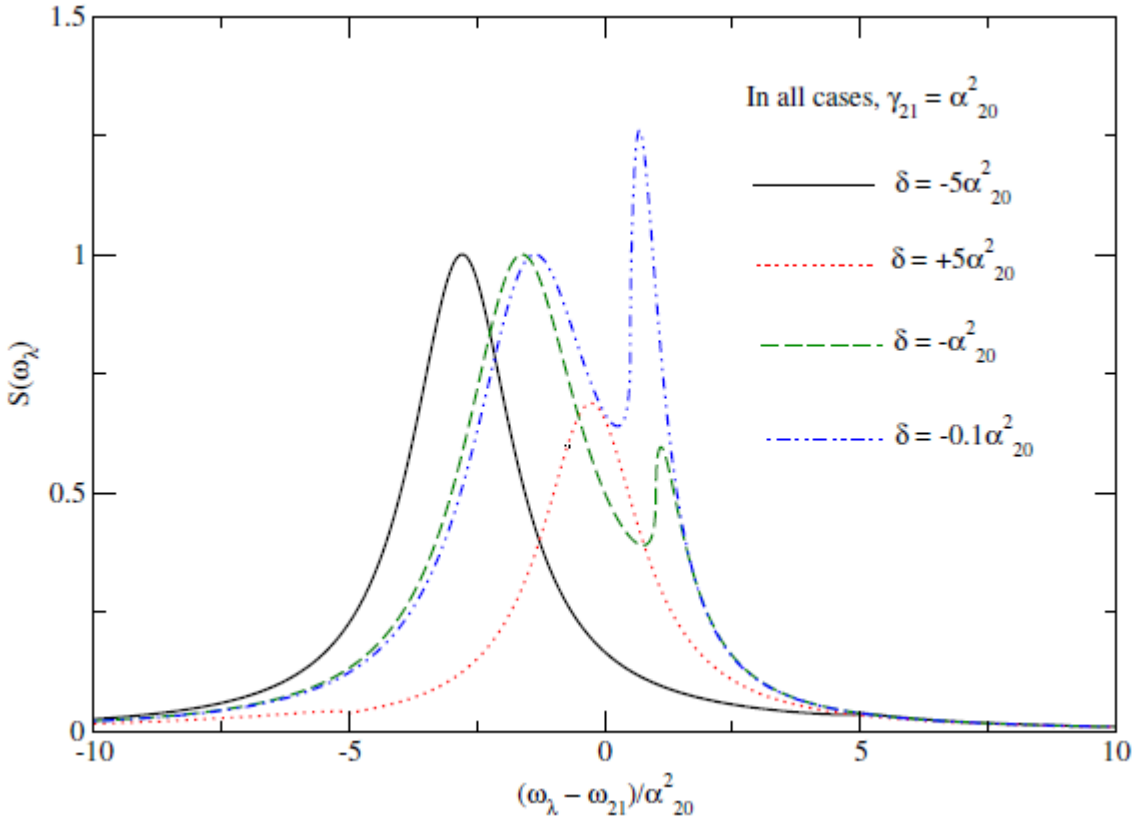

Figure 7. Spectrum of spontaneous emission via |2> −→ |1> for $\gamma_{21} = \alpha^2_{20}$, and for different values of the detuning $\delta = \omega_{20} - \omega_c$ of ω_{20} from ω_c. The frequency ω_{21} for the transition |2>→ |1> is assumed to lie in the photon continuum far outside the gap. The spontaneous emission spectrum splits only for ω_{20} close to the band edge ωc (for $\delta = -\alpha^2_{20}$ and $\delta = -0.1\alpha^2_{20}$), the closer the ω20 to ωc, the more pronounced the splitting. Transitions sufficiently deep inside the gap ($\delta = -5\alpha^2_{20}$) or sufficiently far from the gap ($\delta = +5\alpha^2_{20}$) do not exhibit spectrum splitting

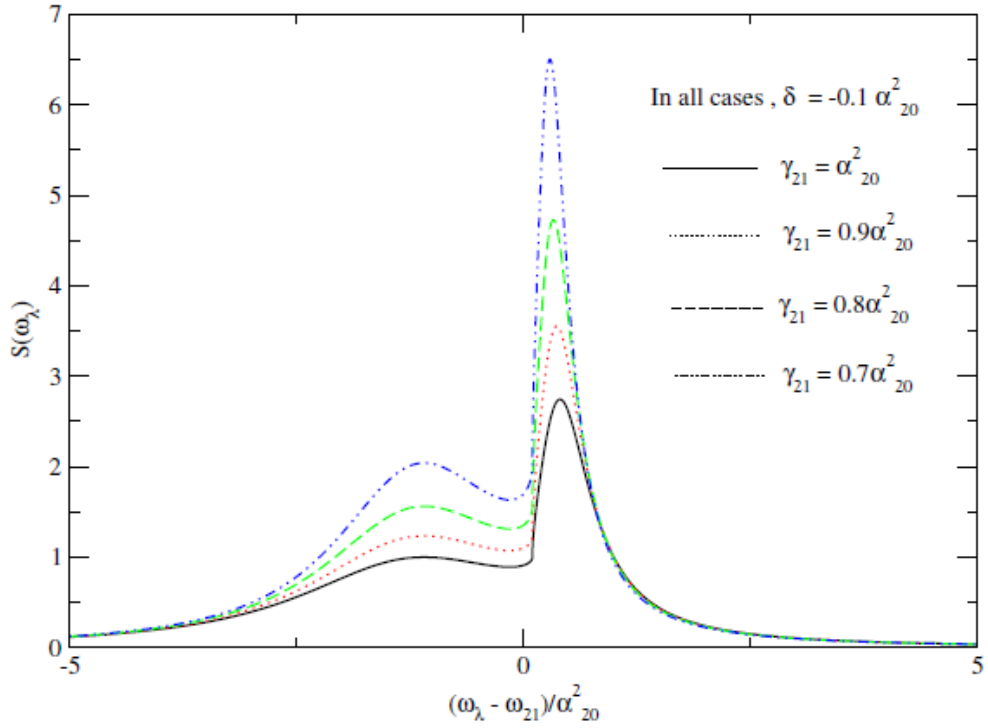

Figure 8. Spectrum of spontaneous emission via $|2\rangle \rightarrow |1\rangle$ for $\delta = \alpha^2_{20}$ and for different values of γ_{21}. The frequency ω_{21} for the transition $|2\rangle \rightarrow |1\rangle$ is assumed to lie in the photon continuum far outside the gap. The smaller the value of γ_{21} the more pronounced the splitting effect on $S(\omega_\lambda)$, though the positions of the peaks is determined only by δ

6. Conclusions

We investigated spontaneous emission from a three-level atom in a Λ configuration embedded in a photonic band gap (PBG) material. Of the two dipole-allowed transitions of the atom, one is near the photonic band edge (the "near" transition), whereas the other one is sufficiently far from the photonic band gap not to be directly affected by the gap (the "far" transition). Though the "far" transition is not directly affected by the photonic band gap, it is indirectly affected by the gap because of its coupling to the "near" transition via the Λ configuration. As a result of this coupling, spontaneous emission through the "far" transition can be used as a probe to measure the strength of the effects of the photonic band gap on spontaneous emission through the "near" transition. In this paper, we showed that the oscillatory behavior as well as the spectrum of the spontaneous emission through the "near" transition are strongly dependent (and, therefore, can be controlled by) the vacuum decay rate of the "far" transition which lies far outside the gap and deep in the photon continuum. In short, we have shown that spontaneous emission through an atomic transition near the edge of a photonic band gap can be investigated by frustrating it by another atomic transition far from the photonic band gap but coupled to the near transition via a Λ configuration.

Appendix A: Derivation of Eq.5.16 for $c_2(t)$: The $\gamma_{21} \neq 0$ Case

The atomic amplitude $c_2(t)$ is obtained from the inverse Laplace transform of $\tilde{c}_2(s+i\delta)$ given by Eq. 5.10 following similar Laplace inversion by Woldeyohannes and John [6]. This inverse Laplace transform is evaluated via the complex inversion formula [27]

$$e^{-i\delta t}c_j(t) = \frac{1}{2\pi i}\int_{\epsilon-i\infty}^{\epsilon+i\infty} e^{st}\tilde{c}_j(s+i\delta)ds \qquad (A.1)$$

where the real number ϵ is chosen so that $s=\epsilon$ lies to the right of all the singularities (poles and branch points) of the function $\tilde{c}_2(s+i\delta)$. It is apparent from Eq. (5.10) that $s=0$ is a branch point of $\tilde{c}_2(s+i\delta)$. In order to evaluate (A1), we consider the contour C shown in Figure 9 where the branch cut of the integrand is chosen to lie along the negative real axis. According to the residue theorem,

$$\frac{1}{2\pi i}\oint_C e^{st}\tilde{c}_2(s+i\delta)ds = R_{\text{sum}} \qquad (A.2)$$

where R_{sum} is the sum of the residues of the integrand at the poles enclosed by the contour C. Omitting the integrands, we obtain

$$\begin{aligned} R_{\text{sum}} &= \frac{1}{2\pi i}\oint_C \\ &= \frac{1}{2\pi i}\left(\int_{AB}+\int_{BDE}+\int_{EH}+\int_{HJK}+\int_{KL}+\int_{LNA}\right). \end{aligned} \qquad (A.3)$$

In the limit $r\rightarrow 0$ and $R\rightarrow\infty$ (so that $T\rightarrow\infty$), the integrals over the curves *BDE*, *HJL* and *LNA* on the *RHS* of Eq. (A1) approach zero and, according to Eq. (5.10), the integral over the line *AB* gives $e^{-i\delta t}c_2(t)$. Therefore,

$$e^{-i\delta t}c_2(t) = R_{\text{sum}} - \lim_{\substack{R\rightarrow\infty \\ r\rightarrow 0}} \frac{1}{2\pi i}\left(\int_{EH}+\int_{KL}\right). \qquad (A.4)$$

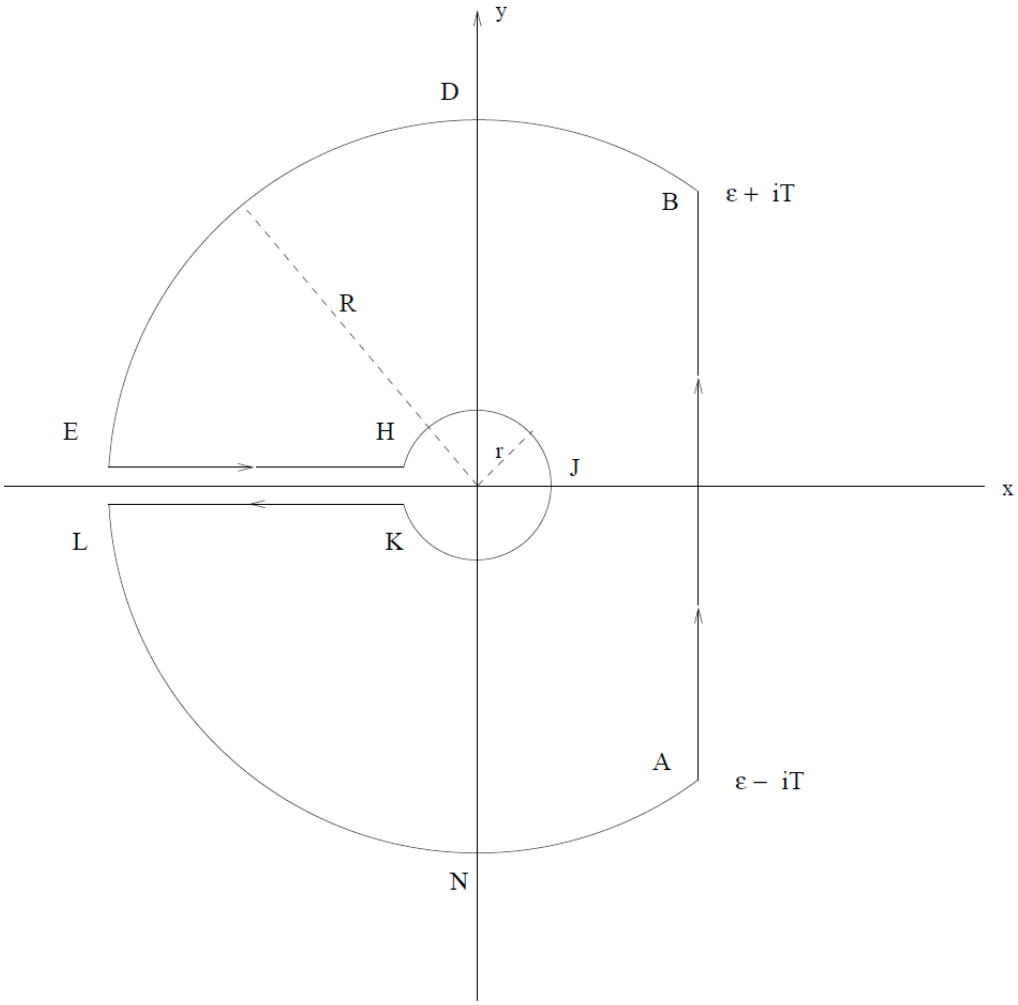

Figure 9. The contour used in the complex inversion formula (A.1)

Along EH, $s = xe^{i\pi} = -x$; and using this in Eq. 5.10 we obtain

$$\lim_{\substack{R\to\infty \\ r\to 0}} \int_{EH} e^{st}\tilde{c}_2(s+i\delta)ds = \int_0^{\infty} \frac{e^{-xt}}{-x-\alpha_{20}e^{-i\pi/4}\sqrt{x}+(\gamma_{21}+i\delta)}dx \tag{A.5}$$

Similarly, along KL, $s = xe^{-i\pi} = -x$; and using this in Eq. 5.10 we obtain

$$\lim_{\substack{R\to\infty \\ r\to 0}} \int_{KL} e^{st}\tilde{c}_2(s+i\delta)ds = -\int_0^{\infty} \frac{e^{-xt}}{-x+\alpha_{20}e^{-i\pi/4}\sqrt{x}+(\gamma_{21}+i\delta)}dx \tag{A.6}$$

Using Eqs. A.5 and A.6 in Eq.A4 we obtain

$$e^{-i\delta t}c_2(t) = R_{\text{sum}} + \frac{\alpha_{20}e^{i\pi/4}}{\pi}\int_0^{\infty} \frac{\sqrt{x}e^{-xt}}{(-x+i\delta+\gamma_{21})^2+i\alpha_{20}^2 x}dx \tag{A.7}$$

Next we evaluate the total residue R_{sum} . From Eq. (5.10), we obtain

$$e^{st}\tilde{c}_2(s+i\delta) = \frac{e^{st}}{(\sqrt{s}-e^{i\pi/4}q_1)(\sqrt{s}-e^{i\pi/4}q_2)} = \frac{e^{st}(\sqrt{s}+e^{i\pi/4}q_1)(\sqrt{s}+e^{i\pi/4}q_2)}{(s-iq_1^2)(s-iq_2^2)} \tag{A.8}$$

Clearly, the function $e^{st}\tilde{c}_2(s+i\delta)$ has simple poles at $s = iq_1^2$ and $s = iq_2^2$. The residues at $s = iq_1^2$ and $s = iq_2^2$ are given by

$$R_1 \equiv \lim_{s\to iq_1^2}(s-iq_1^2)e^{st}\tilde{c}_2(s+i\delta) = \left[\frac{(\sqrt{q_1^2}+q_1)(\sqrt{q_1^2}+q_2)}{q_1^2-q_2^2}\right]e^{iq_1^2 t} \tag{A.9}$$

$$R_2 \equiv \lim_{s\to iq_2^2}(s-iq_2^2)e^{st}\tilde{c}_2(s+i\delta) = \left[\frac{(\sqrt{q_2^2}+q_1)(\sqrt{q_2^2}+q_2)}{q_2^2-q_1^2}\right]e^{iq_2^2 t} \tag{A.10}$$

For the complex roots q_1 and q_2 given by Eq. 5.7, we choose the positive branch of the square root function and

set $\sqrt{q_j^2} = q_j$, $(j = 1, 2)$. The residues at q_1 and q_2 are then given by

$$R_1 = \frac{2q_1}{q_1 - q_2} e^{iq_1^2 t},\ R_2 = \frac{2q_2}{q_2 - q_1} e^{iq_2^2 t} \qquad (A.11)$$

so that the total residue is

$$R_{\text{sum}} = R_1 + R_2 = \frac{2q_1}{q_1 - q_2} e^{iq_1^2 t} + \frac{2q_2}{q_2 - q_1} e^{iq_2^2 t} \qquad (A.12)$$

Using Eq. A.12 in Eq. A.7, we finally obtain Eq. 5.16.

Appendix B: Derivation of Eq. 5.12 for $c_2(t)$: The $\gamma_{21} = 0$ Case

With the initial condition of Eq. 3.4 (that is, atom initially on the upper most level $|2\rangle$), and with the assumption that $\gamma_{21} = 0$ (so that the decay channel $|2\rangle \to |1\rangle$ for the population of level $|2\rangle$ is completely closed), the three-level atom of Figure 1 essentially acts as a two-level atom consisting of levels $|2\rangle$ and $|0\rangle$. In this two-level atom case, the expression for the amplitude $c_2(t)$ is obtained as follows [6].

For $\gamma_{21} = 0$, Eq. 5.16 reduces to

$$D(x) = x^2 + \alpha_{20} x + \delta \qquad (B.1)$$

and its roots are given by

$$u_{1,2} = -\left(\frac{\alpha_{20}}{2}\right) \pm \sqrt{\left(\frac{\alpha_{20}}{2}\right)^2 - \delta} \qquad (B.2)$$

where the upper sign of $\pm$ applies for u_1. Just like in the $\gamma_{21} \neq 0$ case, in the $\gamma_{21} = 0$ case, the amplitude $c_2(t)$ is obtained via the complex inversion formula of Eq. A.1 using the contour of Figure 9. The inversion gives different results depending on the value of the detuning $\delta = \omega_{20} - \omega_c$ of the atomic transition frequency ω_{20} from the band edge frequency ω_c. We consider three different cases, the $\delta < 0$ case (case I), the $0 \le \delta \le (\alpha_{20}/2)^2$ case (case II), and the $\delta > (\alpha_{20}/2)^2$ case (case III).

1. Case I: δ < 0

For $\delta < 0$, the roots of Eq. B.1 are given by

$$\delta < 0 \Rightarrow \begin{cases} u_1 = -\left(\frac{\alpha_{20}}{2}\right) + \sqrt{|\delta| + \left(\frac{\alpha_{20}}{2}\right)^2} \\ u_2 = -\left(\frac{\alpha_{20}}{2}\right) - \sqrt{|\delta| + \left(\frac{\alpha_{20}}{2}\right)^2} \end{cases} \qquad (B.3)$$

In this case, u_1 is a positive real number and, therefore, lies inside the contour of integration so that it has a non-zero residue. On the other hand, u_2 is a negative real number and, therefore, lies outside the contour of integration so that its residue is zero. As a result, when $\delta < 0$, the amplitude $c_2(t)$ is given by

$$\gamma_{21} = 0 \ \&\ \delta < 0$$
$$\Rightarrow c_2(t) = \frac{2u_1}{u_1 - u_2} e^{i(u_1^2 + \delta)t} + I(\delta, t) \qquad (B.4)$$

where

$$I(\delta, t) = \frac{\alpha_{20} e^{i\pi/4}}{\pi} \int_0^\infty \frac{\sqrt{x} e^{-(x - i\delta)t}}{(-x + i\delta)^2 + i\alpha_{20}^2 x} dx \qquad (B.5)$$

and $u_{1,2}$ are given by B.3.

2. Case II: $0 \le \delta \le (\alpha_{20}/2)^2$

In this case

$$0 \le \delta \le (\alpha_{20}/2)^2 \Rightarrow \sqrt{\left(\frac{\alpha_{20}}{2}\right)^2 - \delta} = \sqrt{\left(\frac{\alpha_{20}}{2}\right)^2 - |\delta|}$$

As a result, both roots of Eq. B.1 are negative real numbers given by

$$0 \le \delta \le (\alpha_{20}/2)^2$$
$$\Rightarrow \begin{cases} u_1 = -\left(\frac{\alpha_{20}}{2}\right) + \sqrt{\left(\frac{\alpha_{20}}{2}\right)^2 - |\delta|} < 0 \\ u_2 = -\left(\frac{\alpha_{20}}{2}\right) - \sqrt{\left(\frac{\alpha_{20}}{2}\right)^2 - |\delta|} < 0 \end{cases} \qquad (B.6)$$

and, therefore, lie outside the contour of integration so that their residues are zero. The only contribution to $c_2(t)$ is the branch-cut contribution. The amplitude $c_2(t)$ is then given by

$$\gamma_{21} = 0 \,\&\, 0 \le \delta \le (\alpha_{20}/2)^2 \Rightarrow c_2(t) = I(\delta, t) \qquad (B.7)$$

where $I(\delta, t)$ is given by Eq. B.5.

Case III: $\delta > (\alpha_{20}/2)^2$

In this case,

$$\delta > (\alpha_{20}/2)^2$$
$$\Rightarrow \sqrt{\left(\frac{\alpha_{20}}{2}\right)^2 - \delta} = \sqrt{\left(\frac{\alpha_{20}}{2}\right)^2 - |\delta|} = i\sqrt{|\delta| - \left(\frac{\alpha_{20}}{2}\right)^2}$$

As a result, the roots of Eq. B.1 are complex conjugates of each other and can be expressed in terms of positive real numbers A and B as

$$\delta > (\alpha_{20}/2)^2$$
$$\Rightarrow \begin{cases} v_1 = -A + iB \\ v_2 = -A - iB \end{cases}, \begin{cases} A = \left(\frac{\alpha_{20}}{2}\right) > 0 \\ B = \sqrt{|\delta| - \left(\frac{\alpha_{20}}{2}\right)^2} > 0 \end{cases} \qquad (B.8)$$

so that

$$e^{i(v_1^2 + \delta)t} = e^{i(A^2 - B^2 + \delta)t} e^{2ABt} \to \infty \ (\text{as } t \to \infty) \qquad (B.9)$$

$$e^{i(v_2^2+\delta)t} = e^{i(A^2-B^2+\delta)t}e^{-2ABt} \to 0 \text{ (as } t \to \infty) \quad \text{(B.10)}$$

The residue corresponding to root v_1 increases exponentially in time due to the factor e^{2ABt} and, therefore, is unphysical. As a result, when $\delta > (\alpha_{20}/2)^2$, the amplitude $c_2(t)$ is given by

$$\begin{aligned} &\gamma_{21} = 0 \& \delta > (\alpha_{20}/2)^2 \\ &\Rightarrow c_2(t) = \frac{2v_2}{v_2 - v_1} e^{i(v_2^2+\delta)t} + I(\delta,t) \end{aligned} \quad \text{(B.11)}$$

where $v_{1,2}$ are given by Eq. B.8 and $I(\delta,t)$ is given by Eq. B.5. Summarizing our results for the $\gamma_{21} = 0$ case, we finally obtain

$$\gamma_{21} = 0 \Rightarrow$$

$$c_2(t) = \begin{cases} \dfrac{2u_1}{u_1 - u_2} e^{i(u_1^2+\delta)t} + I(\delta,t), \text{ if } \delta < 0 & (B.12a) \\ I(\delta,t), \text{ if } 0 \le \delta \le (\alpha_{20}/2)^2 & (B.12b) \\ \dfrac{2v_2}{v_2 - v_1} e^{i(v_2^2+\delta)t} + I(\delta,t), \text{ if } \delta > (\alpha_{20}/2)^2 & (B.12c) \end{cases}$$

where

$$u_{1,2} = -\left(\frac{\alpha_{20}}{2}\right) \pm \sqrt{|\delta| + \left(\frac{\alpha_{20}}{2}\right)^2} \quad \text{(B.13a)}$$

$$v_{1,2} = -\left(\frac{\alpha_{20}}{2}\right) \pm i\sqrt{|\delta| - \left(\frac{\alpha_{20}}{2}\right)^2} \quad \text{(B.13b)}$$

the upper signs of $\pm$ applying for u_1 and v_1, and $I(\delta,t)$ is given by Eq. B.5.

4. Steady-state population on level $|2\rangle$ when $\gamma_{21} = 0$

In Eq. B.12a, the exponential $e^{i(u_1^2+\delta)}$ is a non-decaying oscillatory factor because root u_1 (which is given by Eq. B.13a) is a positive real number. On the other hand, in Eq. B.12c the exponential $e^{i(v_2^2+\delta)}$ decays in time like e^{-2ABt} as shown by Eq. B.10. The term $I(\delta,t)$ in Eqs. B.12a-c also decays in time and tends to zero as $t \to \infty$. As a result, in Eqs. B.12a-c for $c_2(t)$, only the first term in Eq. B.12a remains in the long-time limit. Therefore, in the long-time limit, the amplitude $c_2(t)$ is given by

$$\gamma_{21} = 0 \Rightarrow c_2(t) = \begin{cases} \dfrac{2u_1}{u_1 - u_2} e^{i(u_1^2+\delta)t}, \text{ if } \delta < 0 \\ 0, \text{ if } \delta \ge 0 \end{cases} \quad \text{(B.14)}$$

where $u_{1,2}$ are both real and are given by Eq. 13a, the upper sign of $\pm$ applying for u_1. The steady-state population of level $|2\rangle$ is then given by

$$\gamma_{21} = 0 \Rightarrow \lim_{t\to\infty} |c_2(t)|^2 = \begin{cases} \dfrac{4u_1^2}{(u_1 - u_2)^2}, \text{ if } \delta < 0 \\ 0, \text{ if } \delta \ge 0 \end{cases} \quad \text{(B.15)}$$

References

[1] S. John, "Electromagnetic absorption in a disordered medium near a photon mobility edge," *Phys. Rev. Lett.*, 53, 2169 (1984).

[2] S. John, "Strong localization of photons in certain disordered dielectric superlattices," *Phys. Rev. Lett.*, 58, 2486 (1987).

[3] E. Yablonovitch, "Inhibited spontaneous emission in solid-state physics and electronics," *Phys. Rev. Lett.*, 58, 2059 (1987).

[4] S. John and J. Wang, "Quantum electrodynamics near a photonic band gap: photon bound states and dressed atoms," *Phys. Rev. Lett.*, 64, 2418 (1990).

[5] S. John and J. Wang, "Quantum optics of localized light," *Phys. Rev. B*, 43, 12772 (1991).

[6] M. Woldeyohannes and S. John, "Coherent control of spontaneous emission near a photonic band edge: Ph.D Tutorial", *J. Opt. B*, 5, R43-R82 (2003)

[7] S. John and T. Quang, "Spontaneous emission near the edge of a photonic band gap," *Phys. Rev. A*, 50, 1764 (1994).

[8] T. Quang, M. Woldeyohannes, S. John, and G. S. Agarwal, "Coherent control of spontaneous emission near a photonic band edge: a single-atom optical memory device," *Phys. Rev. Lett.*, 79, 5238 (1997).

[9] M. Woldeyohannes and S. John, "Coherent control of spontaneous emission near a photonic band edge: a qubit for quantum computation," *Phys. Rev. A*, 60, 5046 (1999).

[10] M. Boroditsky, R. Vrijen, T. F. Krauss, R. Coccioli, R. Bhat, and E. Yablonovitch, "Spontaneous emission extraction and Purcell enhancement from thin-film 2-D photonic crystals," *J. Lightwave Technol.*, 17, 2096 (1999).

[11] T. Baba, K. Inoshita, H. Tanaka, J. Yoenkura, M. Ariga, A. Matsutani, T. Miyamoto, F. Koyama, and K. Iga, "Strong enhancement of light extraction efficiency in GaInAsP 2-D-arranged micro-columns," *J. Lightwave Technol.*, 17, 2113 (1999).

[12] W. L. Barnes, "Electromagnetic crystals for surface plasmon polaritons and the extraction of light from emissive devices," *J. Lightwave Technol.*, 17, 2170 (1999).

[13] S. Fan, P. R. Villeneuve, and J. D. Joannopoulos, "High extraction efficiency of spontaneous emission from slabs of photonic crystals," *Phys. Ref. Lett.*, 78, 3294 (1997).

[14] C. M. Soukoulis, Ed., "Photonic band gaps and localization," in *Proc. NATO Advanced Research Workshop on Localization and Propagation of Classical Waves in Random and Periodic Media*, Heraklion, Crete, Greece, May 26-30, 1992; see also, *Nato Advanced Studies Institute Series B: Physics*. New York: Plenum, 1993, Vol. 308.

[15] N. M. Lawandy and G. Kweon, "Molecular and free electron spontaneous emission in periodic three- dimensional dielectric structures," in Ref [14].

[16] N. Vats and S. John, "Non-Markovian quantum fluctuations and superradiance near a photonic band edge", *Phys. Rev. A*, 58, 4168 (1998).

[17] S. John and T. Quang, "Photon-hopping conduction and collectively induced transparency in a photonic band gap", *Phys. Rev. A*, 55, 4083 (1995).

[18] M. Woldeyohannes, I. Idehenre, and T. Hardin, "Coherent control of cooperative spontaneous emission from two identical three-level atoms in a photonic crystal", *J. Opt.*, 17, 085105 (2015).

[19] H. Autler and C. H. Townes, "Stark effect in rapidly varying fields," *Phys. Rev.*, 100, 703 (1955).

[20] M. Woldeyohannes, S. John, and V. I. Rupasov, "Resonance Raman scattering in photonic band gap mate- rials," *Phys. Rev. A*, 63, 013814 (2001).

[21] L. Allen and J. H. Eberly, *Optical Resonance and Two-level atoms*. New York: Wiley, 1975.

[22] P. Meystre and M. Sargent, *Elements of Quantum Optics*. New York: Springer-Verlag, 1991.

[23] M.O Scully and S. Zubairy, *Quantum Optics*. London: Cambridge University Press, 1997.

[24] D. F. Walls and G. J. Milburn, *Quantum Optics*. New York: Springer-Verlag, 1995.

[25] W. H. Louisell, *Quantum Statistical Properties of Radiation*. New York: Wiley, 1973.

[26] C. Cohen-Tannoudji, B. Diu and F. Lalo¨e, *Quantum Mechanics, Vol.1*. Toronto: Wiley, 1977.

[27] M. R. Spiegel, *Schaum's Outline of Theory and Problems of Laplace Transforms*. New York: McGraw-Hill, 1965.

[28] J. D. Joannopoulos, R. D. Meade, and J. N. Winn, *Photonic Crystals. Molding the Flow of Light*. Princeton NJ: Princeton University Press, 1995.